Geophysical Research Letters

RESEARCH LETTER
10.1029/2020GL090332

Spatial and Temporal Variability of Brown Carbon in the United States: Implications for Direct Radiative Effects

Nicole A. June[1], Xuan Wang[2], L.-W. Antony Chen[3], Judith C. Chow[4], John G. Watson[4], Xiaoliang Wang[4], Barron H. Henderson[5], Yiqi Zheng[1], and Jingqiu Mao[1]

[1]Department of Chemistry and Biochemistry and Geophysical Institute, University of Alaska Fairbanks, Fairbanks, AK, USA, [2]School of Energy and Environment, City University of Hong Kong, Hong Kong SAR, China, [3]Department of Environmental and Occupational Health, University of Nevada, Las Vegas, NV, USA, [4]Division of Atmospheric Sciences, Desert Research Institute, Reno, NV, USA, [5]Office of Air Quality Planning and Standards, U.S. Environmental Protection Agency, Research Triangle Park, NC, USA

Key Points:
- Model with whitening can largely reproduce spatial and temporal variability of brown carbon in US.
- Biogenic SOA appears to be of minor importance to BrC.
- BrC absorption direct radiative effects appear to be most significant over Arctic region during spring and summer.

Supporting Information:
- Supporting Information S1

Correspondence to:
J. Mao,
jmao2@alaska.edu

Citation:
June, N. A., Wang, X., Chen, L.-W. A., Chow, J. C., Watson, J. G., Wang, X., et al. (2020). Spatial and temporal variability of brown carbon in the United States: Implications for direct radiative effects. *Geophysical Research Letters*, *47*, e2020GL090332. https://doi.org/10.1029/2020GL090332

Received 17 AUG 2020
Accepted 28 OCT 2020
Accepted article online 16 NOV 2020

Abstract A newly developed data set from the Interagency Monitoring of PROtected Visual Environments (IMPROVE) observation network, combined with a 3-D chemical transport model, is used to evaluate the spatial and temporal variability of brown carbon (BrC) in the United States. The model with BrC emitted from biomass burning and biofuel emissions agrees with the seasonal and spatial variability of BrC planetary boundary layer (PBL) absorption aerosol optical depth (AAOD) observations within a factor of 2. The model without whitening, the tendency for absorption to decrease with aerosol aging, overestimates the observed BrC PBL AAOD and does not reflect the measured BrC PBL AAOD spatial variability. The model shows higher absorption direct radiative effects (DRE) from BrC at northern high latitudes than at midlatitudes in spring and summer, due to boreal fire emissions, long whitening lifetimes, and high surface albedos. These findings highlight the need to study BrC over the Arctic region.

1. Introduction

The light-absorbing component of organic aerosols (OA), often referred to as brown carbon (BrC), represents a major uncertainty in current estimates of aerosol radiative forcing. In contrast to black carbon (BC), which absorbs at all visible wavelengths with absorptivity proportional to the inverse of wavelength (Alexander et al., 2008; Bond & Bergstrom, 2006; Kirchstetter et al., 2004), BrC shows much stronger absorptivity at short visible and near-ultraviolet wavelengths. A strong BrC warming effect at the top of the atmosphere (TOA) could be significant compared to the net positive forcing from BC (Arola et al., 2011; Brown et al., 2018; Chung et al., 2012; Feng et al., 2013; Kirchstetter & Thatcher, 2012; Lin et al., 2014; Saleh et al., 2015; Wang et al., 2014; Zhang et al., 2017).

Biomass burning is one of the major sources for BrC, including both primary emissions and secondary formation of humic-like substances (HULIS) (Lack et al., 2012; Laskin et al., 2015). BrC concentrations depend on the fuel and burning conditions for primary emissions (Chen et al., 2010; Chen & Bond, 2010; McClure et al., 2020), as well as chemical changes of the multipollutant mixture between sources and receptors (Cappa et al., 2020; Saleh et al., 2014). Recent studies have found that BrC from residential heating is associated with nitrate-containing OAs (Cappa et al., 2019; Jiang et al., 2019; Zhang et al., 2016). BrC contributions from other anthropogenic sources remain poorly characterized (Lack et al., 2012).

The fate of BrC remains uncertain. Laboratory studies indicate that the BrC absorption lifetime ranges from minutes (Lee et al., 2014; Zhao et al., 2015) to several days (Cappa et al., 2020; Fleming et al., 2020; Lin et al., 2016; Sumlin et al., 2017; Zhong & Jang, 2014). Forrister et al. (2015) found that the BrC absorption in wildfire plumes had a half-life of 9–15 hr, likely due to heterogeneous oxidation, photobleaching, or/and volatilization. These processes are referred as "whitening" in the following sections. An analysis of biomass burning plumes in the Amazon shows a similar lifetime of 1 day (Wang et al., 2016). Even with this short lifetime, BrC can contribute a significant fraction of aerosol radiative forcing in certain regions, including the Arctic (Saleh et al., 2015; Zhang et al., 2017).

BrC observations are lacking. In situ measurements are available from individual field campaigns near ground level (Chen et al., 2010; Hecobian et al., 2010; Zhang et al., 2011, 2013) and from aircraft sampling aloft (Forrister et al., 2015; Wang et al., 2014, 2018; Zeng et al., 2020; Zhang et al., 2017, 2020) with limited spatial and temporal coverage. The Aerosol Robotic Network (AERONET) offers another way to examine BrC through aerosol absorption optical depth (AAOD) using multiband AOD retrievals between 340 and 1,020 nm from direct Sun measurements and single scattering albedo (SSA) derived from sky radiance measurements at several wavelengths (Bahadur et al., 2012; Chen et al., 2019; Chung et al., 2012; Feng et al., 2013; Wang et al., 2016). The AERONET BrC AAOD product is limited by its spatial coverage, data quality, and retrieval assumptions (Schuster et al., 2016). To derive BrC AAOD, AERONET data are processed assuming absorption Ångström exponent (AAE) values for other light-absorbing aerosols such as BC and dust. AAOD measurements below a preset threshold are considered unreliable.

Since January 2016, the Interagency Monitoring of PROtected Visual Environments (IMPROVE) observation network, which measures ground-level aerosol chemical composition across the United States for visibility and air quality purposes, started to acquire and process BrC absorption using a multiwavelength thermal/optical analyzer (Chen et al., 2015; Chow et al., 2015, 2018). This dataset can be used to constrain the mass of BrC and BC and their optical properties.

Global modeling of BrC is still at an early stage, largely due to limited knowledge of emissions, optical properties, chemical compositions, atmospheric transformation, and fate. First, no consensus exists on the global emission inventories of BrC. Several modeling studies estimate emissions using a relative ratio of BrC to organic carbon (OC) from BB and biofuel combustion, but this ratio varies from 25% to 100% among different studies (Feng et al., 2013; Lin et al., 2014; Saleh et al., 2015; Wang et al., 2014). Second, measured optical properties of BrC, particularly the imaginary part of aerosol refractive index (RI), vary widely (Wang et al., 2014). BrC consists of a range of poorly characterized organic compounds with absorptivities and volatilities spanning several orders of magnitude (Saleh et al., 2014). Lastly, there is no consensus on the fate of BrC (Cappa et al., 2020; Wang et al., 2018; Zhao et al., 2015). Modeling studies suggest that one of the largest uncertainties in their estimates is the absence of a continuous BrC observational network.

Here we use the OC, EC, and BrC data processed from the IMPROVE observation network (153 sites) in the year of 2016, combined with a global chemical transport model (GEOS-Chem), to examine the spatial and temporal variability of BrC in the United States. The concurrent constraints on aerosol mass and optical properties in a 3-D model provide an unprecedented opportunity to examine source contributions, distributions, lifetimes, and radiative impacts of BrC in the United States and likely elsewhere.

2. Observations and Model

2.1. Observational Data Set

The 2016 IMPROVE data set contains concentrations of $PM_{2.5}$ IMPROVE OC, EC, total carbon (TC = OC + EC), and BrC absorption for 17,390 filter samples from 153 monitoring locations representing regional-scale National Parks and Wilderness areas. Light absorption coefficients at seven wavelengths (i.e., 405, 445, 532, 635, 780, 808, and 980 nm) are apportioned to BC and BrC following a two component model with correction for aerosol filter loading (Chen et al., 2015, 2019; Chow et al., 2015). The mass absorption coefficients (MAC) for both BC and BrC are also established for each of the seven wavelengths by reconciling the BC and BrC absorptions (Abs_{BC} and Abs_{BrC}) with TC values. This results in MAC_{BrC} of 3.9, 2.0, and 0.8 $m^2\,g^{-1}$ and MAC_{BC} of 13.2, 10.9, and 8.8 $m^2\,g^{-1}$ for 365, 440, and 550 nm, respectively. With these empirically derived MACs, BC, BrC, and non-light-absorbing OC (i.e., TC-BC-BrC) mass concentrations are calculated for each sample. BC derived by this method agrees well with EC quantified by the IMPROVE_A carbon analysis protocol (Chen et al., 2015; Chow et al., 2007). Taking non-light-absorbing OC into account, the average MAC_{OA} are 0.81, 0.41, and 0.18 $m^2\,g^{-1}$ at 365, 440, and 550 nm respectively, in agreement with field observations (Table S3 in the supporting information) and a recent review by Saleh (2020). This dataset does not address the effect of relative humidity on OC optical properties or the aging of BrC on filters as they are stored under refrigeration <4°C.

The planetary boundary layer (PBL) absorption aerosol optical depth (AAOD) from observations for each site is calculated as

$$AAOD_{BrC,\lambda} = MAC_{BrC,\lambda} \times Mass_{BrC} \times PBL_{Height}, \quad (1)$$

where $MAC_{BrC,\lambda}$ is the derived MAC for BrC at wavelength λ ($m^2\ g^{-1}$) and $Mass_{BrC}$ is the derived BrC mass concentrations in g m^{-3}. PBL_{Height} is the monthly average boundary layer height obtained from the model. The AAOD for BC is calculated in a similar way. As PBL AAOD is based on $MAC_{BrC,\lambda} \times Mass_{BrC}$, a quantity directly obtained from multiwavelength absorption measurements, this metric is used for the following comparison to minimize uncertainties in the two component model. The uncertainties associated with BrC AAOD observations are estimated to be 33% on annual mean basis, consistent with Chung et al. (2012).

2.2. Model

We run GEOS-Chem v11.1.0 coupled with the Rapid Radiative Transfer model for GCMs (RRTMG) module (Heald et al., 2014). GEOS-Chem is a global 3-D chemical transport model driven by assimilated meteorological observations from the Goddard Earth Observing System (MERRA-2) of the NASA Global Modeling and Assimilation Office (GMAO) (www.geos-chem.org). The MERRA-2 meteorological data have 3-hr temporal resolution (1 hr for surface variables and mixing depths) with 0.5° × 0.625° horizontal resolution and 72 vertical layers from the surface to 0.01 hPa. We regrid the meteorological data to 2° × 2.5° horizontal resolution and 47 vertical layers for GEOS-Chem input. Previous analyses show that he MERRA-2 field provides reasonable PBL height (Molod et al., 2019). The model reads in a multiwavelength 8-day average surface albedo that is constructed from MODIS land albedo data (MCD43C3) (Heald et al., 2014).

GEOS-Chem simulates aerosol mass concentrations for sulfate-nitrate-ammonium (Park et al., 2004), size-resolved mineral dust (Duncan Fairlie et al., 2007), fine and coarse sea salt (Alexander et al., 2005), and OC (Park et al., 2003). GEOS-Chem assumes external mixing for all aerosols, with hygroscopic growth factors dependent on local relative humidity. Biomass burning emissions of BC and primary organic aerosols (POA) use the year-specific daily mean GFED v4.1 (Global Fire Emissions Database) inventory for the year of 2016 (Giglio et al., 2013; van der Werf et al., 2010) (Figures S11). Anthropogenic emissions use the EPA National Emissions Inventory (NEI11v1) for the United States (EPA NEI, 2015). The sector of biofuel emissions is separated from total emissions for this study. All NEI emissions were scaled to 2013 using nation-wide scaling factors, as 2013 is the closest available year out of the available range (2006–2013). POA emissions from these sources are processed in the model. Secondary organic aerosols (SOA) are adopted from GEOS-Chem v12.1 with a simple scheme that includes SOA formation from isoprene, monoterpenes, biomass burning, and fossil fuel, as detailed by Pai et al. (2020).

The GEOS-Chem model has been used to study BrC on regional and global scales (Jo et al., 2016; Park et al., 2010; Wang et al., 2014, 2016, 2018). This study follows Wang et al. (2018), with explicit treatment of BrC emissions from biomass burning and biofuel emissions. This model has been evaluated against several aircraft measurements over the United States (SEAC4RS and DC3) and elsewhere (ARCTAS, EUCAARI, and HIPPO) (Wang et al., 2014, 2018). Instead of separating BrC from non-light-absorbing carbon, we assign absorption properties to OA with the assumption that OA absorption (Abs_{OA}) results exclusively from BrC absorption (Abs_{BrC}). BrC absorption is computed as

$$Abs_{BrC} = Abs_{OA} = MAC_{OA} \times Mass_{OA} = MAC_{BrC} \times Mass_{BrC}. \quad (2)$$

Thus, BrC represents a fraction of OA, and only MAC_{OA} is computed. MAC_{OA} and its wavelength dependence can be computed as a function of BC/OA ratio (Saleh et al., 2014):

$$k_{OA,\,550\ \mathrm{nm}} = 0.016 \log_{10}\left(\frac{BC}{OA}\right) + 0.04, \quad (3)$$

$$w = \frac{0.21}{\frac{BC}{OA} + 0.07}, \quad (4)$$

$$k_{OA} = k_{OA,\,550\ \mathrm{nm}} \left(\frac{550}{\lambda}\right)^{w} \quad (5)$$

where $k_{OA,550\ nm}$ is the imaginary RI for OA at 550 nm, k_{OA} is the imaginary RI at wavelength λ, and w is the wavelength dependence of imaginary RI. w is different from AAE, as w is only related to RI and AAE is related to other factors such as aerosol size distribution and density. MAC values at wavelength λ can be computed using Mie theory following Wang et al. (2018). Assuming BC/OA emission ratios of 0.05 for biomass burning and 0.12 for biofuel, MAC_{OA} for biomass burning emissions are 1.33, 0.77, and 0.35 $m^2\ g^{-1}$ for 365, 440, and 550 nm, respectively; MAC_{OA} for biofuel emissions are 1.19, 0.76, and 0.39 $m^2\ g^{-1}$ for 365, 440, and 550 nm, respectively. These values are consistent with the values from Wang et al. (2018). These MAC values differ from MAC values from IMPROVE observations that are based on total OA mass rather than BrC mass. SOA is assumed to be nonabsorbing, as Wang et al. (2018) finds that anthropogenic SOA contributes little to absorption in the United States, and laboratory studies find biogenic SOA to be nonabsorbing (He et al., 2018). The aromatic anthropogenic SOA could play a more important role for regions where aromatic emissions are high (Zhang et al., 2020). The lensing effect appears to be small (Cappa et al., 2020) and is not explicitly treated.

BrC whitening follows the description by Wang et al. (2018):

$$Abs_{BrC,\,t+\Delta t} = Abs_{BrC,\,t} \cdot \exp\left(-\frac{[OH]\cdot\Delta t}{5\times 10^5}\right). \tag{6}$$

BrC absorption decreases as a function of ambient OH concentrations. The whitening scheme also assumes that BrC absorption remains constant after it drops to 25% of its initial value. This results in a whitening lifetime of 0–3 days in summer and 3–10 days in winter, with a strong latitude gradient resulting from solar radiation intensity (Figure S2). The model-estimated whitening lifetime appears to be longer than that from several laboratory studies (Lee et al., 2014; Zhao et al., 2015), but it is comparable to others (Cappa et al., 2020; Fleming et al., 2020; Li et al., 2019; Lin et al., 2016; Sumlin et al., 2017; Zhong & Jang, 2014).

3. Results

3.1. Model Evaluation for OC and EC

Figure 1 compares the monthly averaged modeled and observed OC mass concentrations for four regions of the continental United States (NE, SE, NW, and SW). Observed OC peaks during summer and fall in the NE, NW, and SW regions and peaks during fall in the SE region. To a large extent, this is driven by wildfire emissions (Carter et al., 2020), as shown in Figure S10. In particular, Southern Appalachian Fires occurred from October to December 2016 in Georgia and North Carolina due to abnormal drought, leading to OC peaks during fall in this region. OC shows another peak during winter in the NE, which is largely attributed to biofuel emissions in this region. In general, the model can reasonably reproduce the magnitude and annual cycle of OC in the NW and SW, with SOA contributing to 30–50% of OC. However, the model tends to overestimate IMPROVE OC by a factor of 2 throughout the year for the NE and SE regions, largely due to high SOA production. Compared to observed OC, the modeled POC has a negative normalized mean bias (NMB) throughout all seasons and regions, with −31% in the NE, −29% in the NW, −32% in the SE, and −57% in the SW (Table S2). The following analyses compare the observed OC with modeled primary OC (POC) and discuss the potential role of SOA contributions to BrC. The model reproduces the observed seasonality and magnitude of EC (Figures S7 and S8), lending confidence in model representation of BC optical properties in this work.

3.2. Model Evaluation of BrC Absorption

As model estimates and measurements are based on different assumptions of MAC values (MAC_{OA} vs. MAC_{BrC}), it is impractical to compare modeled versus observed BrC on a concentration basis. The PBL AAOD is used for this comparison, which is directly observed from IMPROVE network and independent on MAC assumptions. Comparing to total column AAOD, PBL AAOD has several advantages. It minimizes the influence from BrC in the free troposphere, which is not well constrained by the IMPROVE data set; it also removes the influence of seasonal variations in PBL height, allowing comparison of BrC absorption and radiative impacts between different seasons. The total column BrC AAOD is higher than PBL AAOD by 30–50%. The comparison on surface AAOD is shown in Figure S1, consistent with Figure 2.

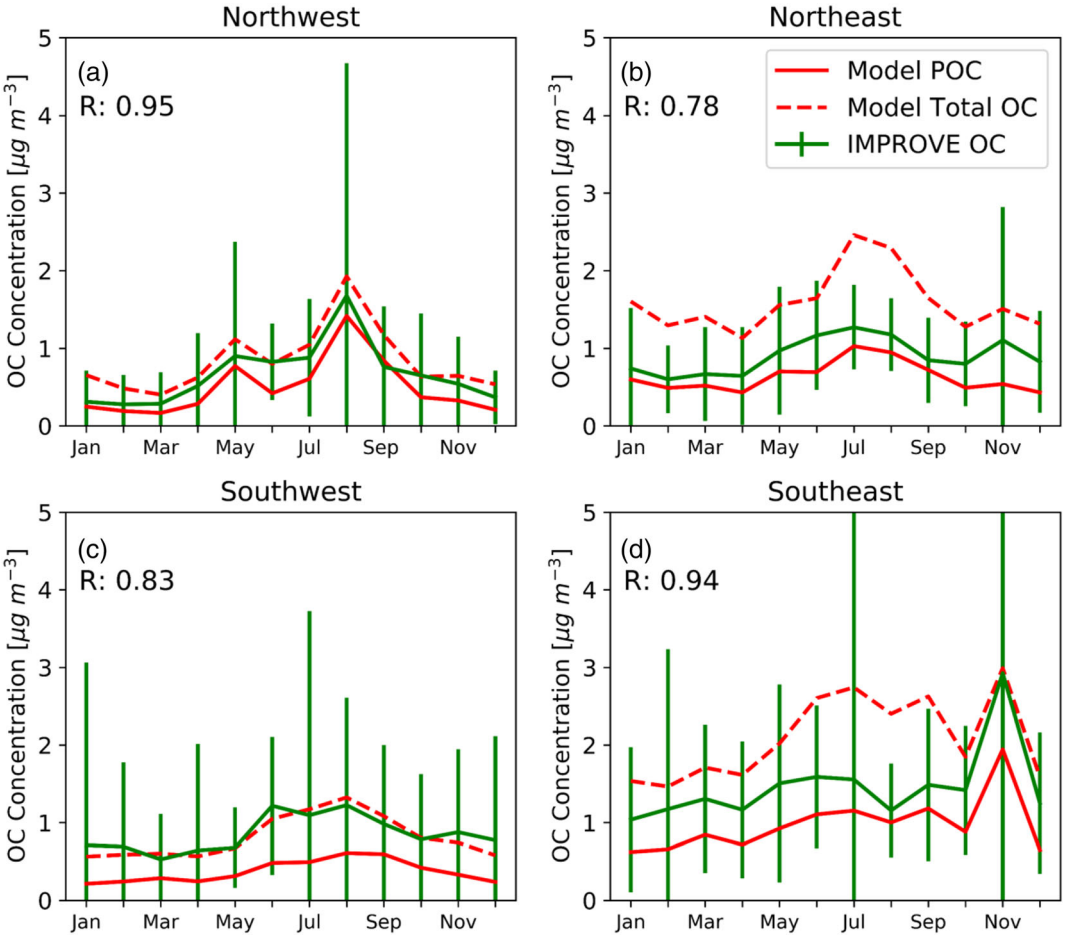

Figure 1. Monthly averaged observed (green) organic carbon (OC) concentrations and modeled (red) primary OC (POC) at observation sites defined by the quadrants created by the 40°N latitude line and the 90°W longitude line. The observed OC is directly measured following the IMPROVE_A carbon analysis protocol. Error bars represent the monthly standard deviation of the OC observations. The red dashed line is the modeled total OC with both POC and SOA contributions. *R* values are the Pearson correlation coefficients between the model POC and the IMPROVE observations.

Figure 2 shows the modeled and observed BrC PBL AAOD at 365 nm for 2016, with NMB and normalized mean error (NME) for each region and season described in Table S1. The comparisons at 440 and 550 nm are shown in Figures S3 and S4, respectively. Observations show stark differences between the western and eastern United States. First, the eastern United States shows higher BrC AAOD than the west in most seasons (winter, spring, and fall), likely due to its higher biofuel and biomass burning emissions. However, maxima of BrC AAOD are found in the western U.S. during summer, which are mainly attributed to wildfires. Figure 2 also shows that the eastern United States shows higher BrC AAOD in winter than in summer, which could be explained by the seasonal variations of emissions and whitening lifetimes, including the Southern Appalachian Fires in Southeast United States during fall and winter. Another important feature from observations is that the BrC PBL AAOD shows a minimum in the SE United States during summer, when observed OC levels reach their maxima in summer and when biogenic SOA are likely predominant (Ridley et al., 2018), suggesting a minor contribution of biogenic SOA to BrC.

The model reproduces the spatial and temporal patterns of BrC AAOD at 365 nm over the Continental United States (CONUS), as shown in Figure 2. The model run with whitening has a NMB of 41% in the NE, 87% in the NW, 20% in the SE, and −35% in the SW. Detailed statistics on these comparisons are tabulated in Table S1. Since the model only assumes BrC from biomass burning and biofuel emissions, this agreement supports the hypothesis that biomass burning and biofuel emissions account for the majority of BrC on a regional basis, and biogenic SOA may play a relatively minor role in BrC concentrations. The model tends

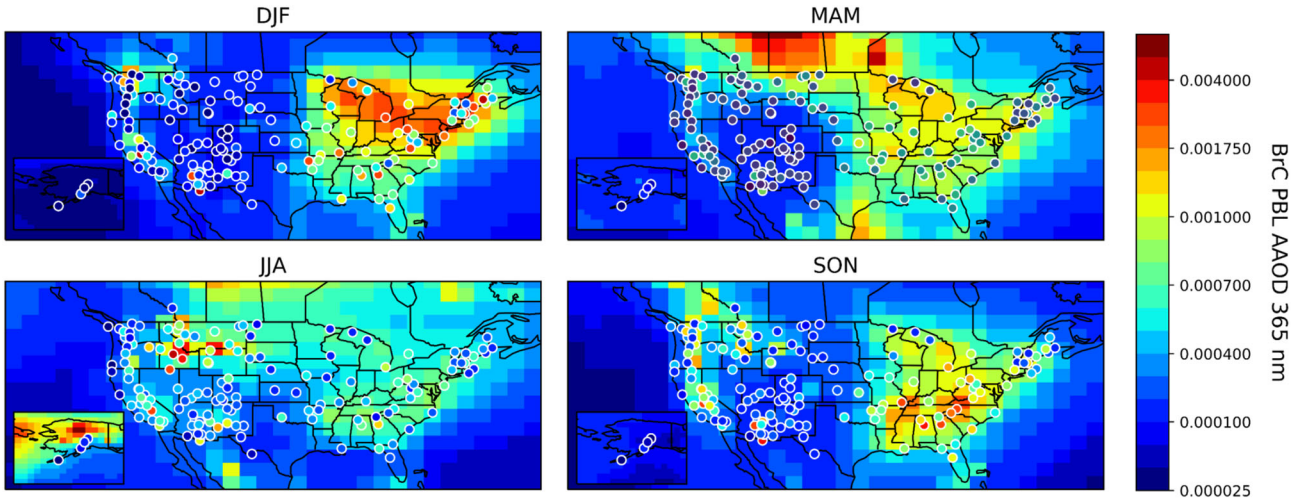

Figure 2. BrC aerosol absorption optical depth in the planetary boundary layer (PBL AAOD) at 365 nm averaged by season for 2016. The background grid is the GEOS-Chem modeled output, and circles are BrC observations from IMPROVE sites. The four seasons are winter: December to February (DJF); spring: March to May (MAM); summer: June to August (JJA); and fall: September to November (SON). Detailed statistics on the comparison, grouped by season and region, are described in Table S1.

to underestimate observed BrC AAOD in the western United States during summer and the northern United States during spring, likely due to uncertainties in biomass burning emissions and/or optical properties, and model representation errors (i.e., the model tends to have too much numerical diffusion for plumes) (Eastham & Jacob, 2017). Lastly, the model tends to overestimate observations in Alaska during summer, mainly because these IMPROVE sites are rarely exposed to interior boreal forest fires while model results are heavily influenced by numerical diffusion of these fire plumes (Potter & Conkling, 2017).

3.3. BrC Whitening Lifetime

Figure 3 compares BrC PBL AAOD at 365 nm between observations and two model runs: with and without whitening. The model without whitening tends to overestimate BrC PBL AAOD in spring, fall, and winter by more than a factor of 2, exceeding the measurement uncertainties of BrC (28–37%). Similar results are found in Table S1, where NMB and NME are significantly improved for the model with whitening in most regions and seasons. These statistics indicate that the model with whitening better represents the observations.

The short whitening lifetime of BrC is consistent with the large spatial variability revealed by the IMPROVE observations (Figure 2). For example, in Figure 2, the model with whitening successfully captures the observed spatial variability in the SE United States during fall (SON panel). However, this feature is not found in the model without whitening (Figure S6). As those high BrC AAOD measurements are not propagating to the nearby sites, whitening suppresses the wide spreading of BrC absorption and enhances its spatial variability.

3.4. Seasonal Variation of BrC Absorption Direct Radiative Effect

With a reasonable agreement on BrC AAOD, the direct radiative effect (DRE) due to BrC absorption can be estimated for different seasons. Similar to Wang et al. (2018), the global BrC absorption DRE computed for 2016 is 0.04 W/m^2, lower than the estimate of 0.13 W/m^2 by Brown et al. (2018) and the 0.10 W/m^2 by Zhang et al. (2020).

Figure 4 shows the all-sky absorption DRE at the TOA only due to BrC absorption over the CONUS and lower Arctic Circle. This is calculated as the difference between the DRE from total OA from the base run and the DRE from total OA in the model run excluding BrC absorption. The resulting difference is thus only due to BrC absorption. As shown in Figure 4, the absorption DRE of BrC shows significant seasonal variation, with enhancement in the NE during winter, in the NW in summer, and the SE in fall. These effects are driven by both the strength in biomass burning and biofuel emissions and the BrC whitening lifetime (Figure S2). The impact of BrC absorption in CONUS appears to be mainly local, limited in source

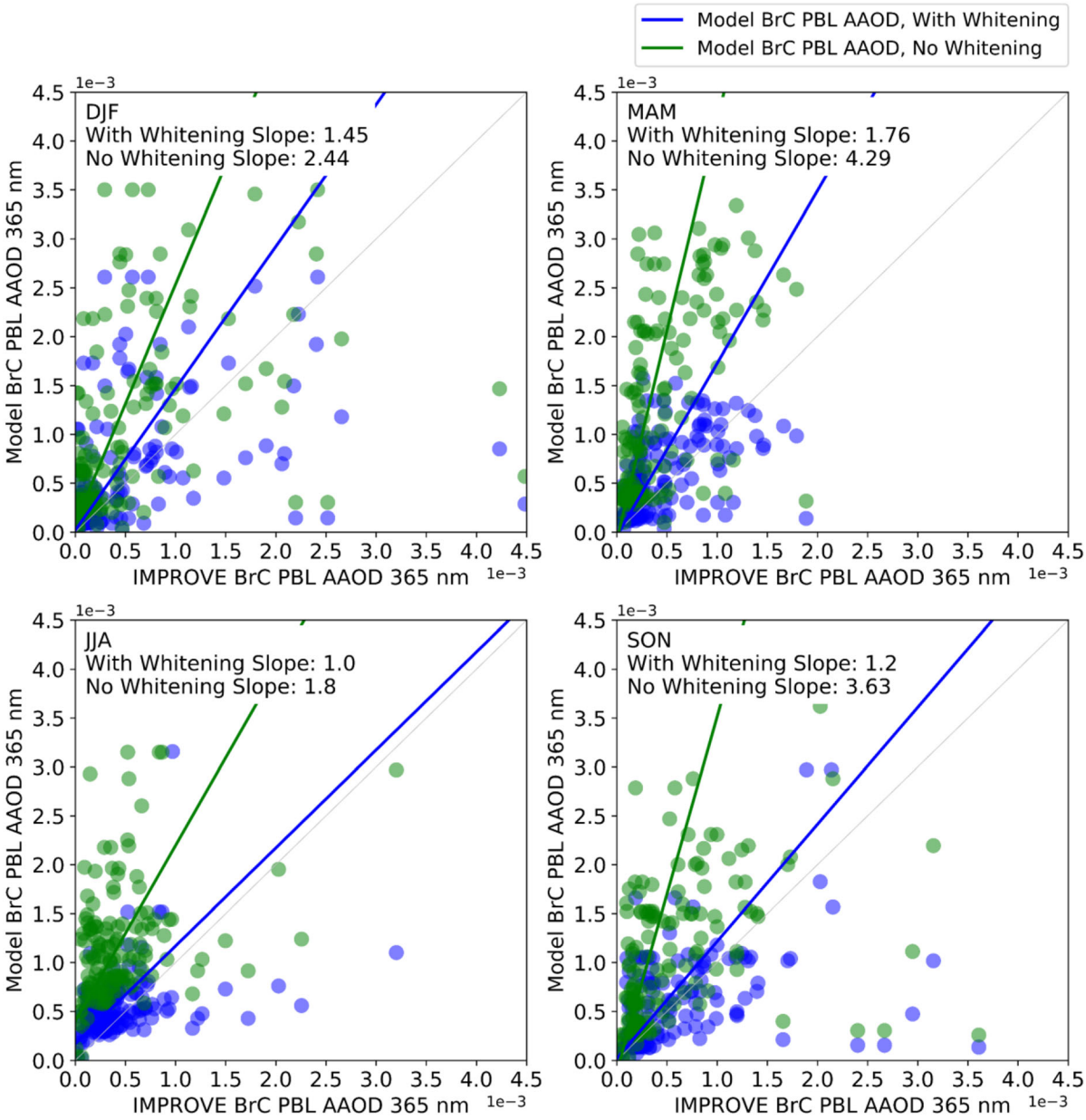

Figure 3. Comparisons of BrC PBL AAOD at 365 nm with whitening (blue) and without whitening (green) for four seasons (DJF, MAM, JJA, and SON). Reduced major axis regressions are shown as solid lines, with confidence level (0.95) and fit equations implemented following Warton et al. (2006) for limiting the influence of outliers. The linear regression slopes are displayed on each plot.

regions. In contrast, BrC absorption DREs show higher and more widespread impacts over the northern high latitude, particularly during summer and spring, consistent with recent global survey of BrC (Zeng et al., 2020) and global model studies (Brown et al., 2018; Zhang et al., 2020).

The high-absorption BrC DREs at northern high latitudes during summer and spring are due to several reasons. First, boreal forest fires become active in spring and reach maximum in summer, with little activity in other seasons. The western Arctic is also exposed to biomass burning contributions from Siberia during spring (Warneke et al., 2009), as shown in Figure S10. Second, boreal forest fire emissions tend to have higher OC contents relative to BC, in contrast to midlatitudes where savanna, grass, shrub, and agricultural burning have lower emission factors of OC relative to BC. It is also shown in Figure 4 that BrC can account for over 50% of BC + BrC warming at northern high latitudes during summer and spring when boreal forest

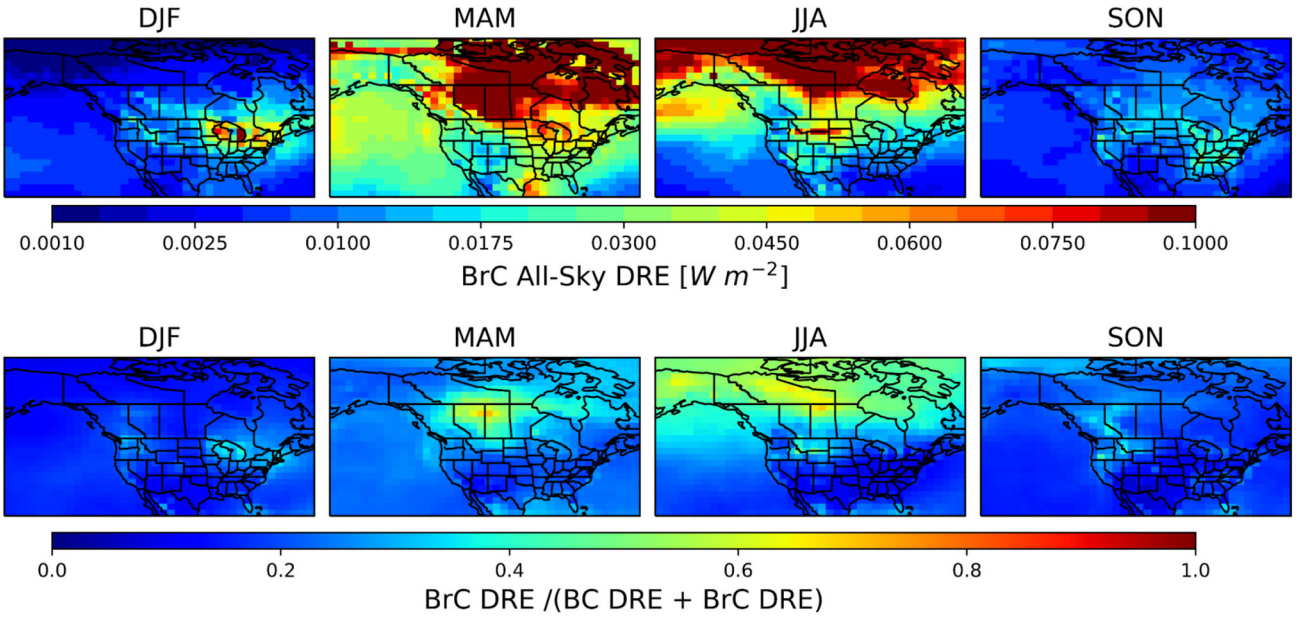

Figure 4. (Upper) Seasonal averaged BrC all-sky absorption direct radiative effect (DRE) computed by the GEOS-Chem model for the year of 2016. (Lower) Seasonal averaged ratio of BrC all-sky absorption DRE and the combined all-sky absorption DRE of BrC and BC. The four seasons are winter: December to February (DJF); spring: March to May (MAM); summer: June to August (JJA); and fall: September to November (SON).

fires are most active, but to a lesser extent during fall and winter. Third, BrC shows longer whitening lifetimes at high latitudes than that at midlatitudes (Figure S2). The BrC whitening lifetime can reach 3–7 days in spring at high latitudes, while it is less than 1 day at midlatitudes. This difference in lifetime allows further wide spreading of BrC DRE. Fourth, BrC absorption DRE is amplified by high surface albedos due to surface snow at northern high latitudes in the spring (Arola et al., 2015). As a result, BrC absorption DRE in spring is as significant as that in summer at high latitudes, despite lower emissions from boreal forest fires in spring than in summer. In fact, the BrC absorption DRE during spring can exceed the scattering DRE of OAs during spring, leading to a net warming from OAs at northern high latitudes (Figure S9). Additional field observations are needed to evaluate model results in this region.

4. Discussion

A new observational data set from the IMPROVE network is combined with a 3-D chemical transport model to evaluate the spatial and temporal variability of BrC in the United States. This data set provides concurrent constraints on both aerosol mass and optical properties. The model with only BrC emitted from biomass burning and biofuel emissions can largely reproduce the seasonal and spatial variability of BrC PBL AAOD from observations, within a factor of 2. This suggests that biomass burning and biofuel emissions may contribute most of the BrC in the United States, while biogenic SOA appears to be of minor importance to BrC (Flores et al., 2014; He et al., 2018; Lambe et al., 2013). The model without whitening tends to overestimate the observed BrC PBL AAOD nor does it reflect the spatial variability of BrC PBL AAOD that is driven by the relative short BrC lifetime. The model suggests higher absorption DREs from BrC at northern high latitudes than at midlatitudes in spring and summer, due to boreal fire emissions, long whitening lifetime, and high surface albedo.

Despite the reasonably good agreement of BrC PBL AAOD between observations and the model with whitening, large uncertainties remain to be resolved. First, filter-based observations do not address the effect of relative humidity on OC and its optical properties, while the model computes AAOD at ambient conditions. Modeled BrC PBL AAOD can be reduced by 40–60% when dry aerosols are assumed for AAOD calculations. How to apply humidity dependence for both model and filter-based observations requires further investigation. Second, the IMPROVE data set only provides constraints on the surface and PBL BrC over a limited longitude and latitude range. The BrC formed in the free troposphere is not well constrained and requires further evaluation from aircraft measurements (Zeng et al., 2020; Zhang et al., 2017). Third, other

photochemical aging mechanism, such as nighttime processing (Cheng et al., 2020; Li et al., 2019) and NO_x modulation (He et al., 2018), are not taken into account in this work. These uncertainties warrant future studies on BrC from laboratory, field observations, and modeling. As wildfires become more and more intense due to global warming, the Arctic and northern high latitudes may deserve particular attention, where BrC absorption DRE appears to be most significant.

Data Availability Statement

The IMPROVE OC and EC data are available at IMPROVE website (http://vista.cira.colostate.edu/Improve/data-page/). Processed BrC data and model output can be accessed online (at https://figshare.com/articles/dataset/BrC_Observation_and_Model_for_United_States/13048337).

Acknowledgments

J. Mao and L.-W. A. Chen acknowledge the support from NSF Grants AGS-2026821 and AGS-2026824. The brown carbon scheme development in GEOS-Chem was supported by the EPA-STAR program (Grant RD-83503301 to C. L. Heald at MIT). Although the research described in this article was funded in part by the U.S. EPA, it has not been subjected to the EPA's required peer and policy reviews and therefore does not necessarily reflect the views of the EPA, and no official endorsement should be inferred. This research is partially funded by the UAF Faculty Initiative Fund, as well as the REU Site: Understanding Arctic as a System (Grant NSF-OPP-1560372). The authors would like to acknowledge C. Holmes (Florida State) on regression code.

References

Alexander, B., Park, R. J., Jacob, D. J., Li, Q. B., Yantosca, R. M., & Savarino, J. (2005). Sulfate formation in sea-salt aerosols: Constraints from oxygen isotopes. *Journal of Geophysical Research*, *110*, D10307. https://doi.org/10.1029/2004JD005659

Alexander, D. T. L., Crozier, P. A., & Anderson, J. R. (2008). Brown carbon spheres in East Asian outflow and their optical properties. *Science*, *321*(5890), 833–836. https://doi.org/10.1126/science.1155296

Arola, A., Schuster, G., Myhre, G., Kazadzis, S., Dey, S., & Tripathi, S. N. (2011). Inferring absorbing organic carbon content from AERONET data. *Atmospheric Chemistry and Physics*, *11*(1), 215–225. https://doi.org/10.5194/acp-11-215-2011

Arola, A., Schuster, G. L., Pitkänen, M. R. A., Dubovik, O., Kokkola, H., Lindfors, A. V., et al. (2015). Direct radiative effect by brown carbon over the Indo-Gangetic Plain. *Atmospheric Chemistry and Physics*, *15*(22), 12,731–12,740. https://doi.org/10.5194/acp-15-12731-2015

Bahadur, R., Praveen, P. S., Xu, Y., & Ramanathan, V. (2012). Solar absorption by elemental and brown carbon determined from spectral observations. *Proceedings of the National Academy of Sciences*, *109*(43), 17,366–17,371. https://doi.org/10.1073/pnas.1205910109

Bond, T. C., & Bergstrom, R. W. (2006). Light absorption by carbonaceous particles: An investigative review. *Aerosol Science and Technology*, *40*(1), 27–67. https://doi.org/10.1080/02786820500421521

Brown, H., Liu, X., Feng, Y., Jiang, Y., Wu, M., Lu, Z., et al. (2018). Radiative effect and climate impacts of brown carbon with the Community Atmosphere Model (CAM5). *Atmospheric Chemistry and Physics*, *18*(24), 17,745–17,768. https://doi.org/10.5194/acp-18-17745-2018

Cappa, C. D., Lim, C. Y., Hagan, D. H., Coggon, M., Koss, A., Sekimoto, K., et al. (2020). Biomass-burning-derived particles from a wide variety of fuels—Part 2: Effects of photochemical aging on particle optical and chemical properties. *Atmospheric Chemistry and Physics*, *20*(14), 8511–8532. https://doi.org/10.5194/acp-20-8511-2020

Cappa, C. D., Zhang, X., Russell, L. M., Collier, S., Lee, A. K. Y., Chen, C.-L., et al. (2019). Light absorption by ambient black and brown carbon and its dependence on black carbon coating state for two California, USA, cities in winter and summer. *Journal of Geophysical Research: Atmospheres*, *124*, 1550–1577. https://doi.org/10.1029/2018JD029501

Carter, T. S., Heald, C. L., Jimenez, J. L., Campuzano-Jost, P., Kondo, Y., Moteki, N., et al. (2020). How emissions uncertainty influences the distribution and radiative impacts of smoke from fires in North America. *Atmospheric Chemistry and Physics*, *20*(4), 2073–2097. https://doi.org/10.5194/acp-20-2073-2020

Chen, L. W. A., Chow, J. C., Wang, X. L., Robles, J. A., Sumlin, B. J., Lowenthal, D. H., et al. (2015). Multi-wavelength optical measurement to enhance thermal/optical analysis for carbonaceous aerosol. *Atmospheric Measurement Techniques*, *8*(1), 451–461. https://doi.org/10.5194/amt-8-451-2015

Chen, L.-W. A., Verburg, P., Shackelford, A., Zhu, D., Susfalk, R., Chow, J. C., & Watson, J. G. (2010). Moisture effects on carbon and nitrogen emission from burning of wildland biomass. *Atmospheric Chemistry and Physics*, *10*(14), 6617–6625. https://doi.org/10.5194/acp-10-6617-2010

Chen, S., Russell, L. M., Cappa, C. D., Zhang, X., Kleeman, M. J., Kumar, A., et al. (2019). Comparing black and brown carbon absorption from AERONET and surface measurements at wintertime Fresno. *Atmospheric Environment*, *199*, 164–176. https://doi.org/10.1016/j.atmosenv.2018.11.032

Chen, Y., & Bond, T. C. (2010). Light absorption by organic carbon from wood combustion. *Atmospheric Chemistry and Physics*, *10*(4), 1773–1787. https://doi.org/10.5194/acp-10-1773-2010

Cheng, Z., Atwi, K. M., Yu, Z., Avery, A., Fortner, E. C., Williams, L., et al. (2020). Evolution of the light-absorption properties of combustion brown carbon aerosols following reaction with nitrate radicals. *Aerosol Science and Technology*, 1–15. https://doi.org/10.1080/02786826.2020.1726867

Chow, J. C., Wang, X., Sumlin, B. J., Gronstal, S. B., Chen, L.-W. A., Trimble, D. L., et al. (2015). Optical calibration and equivalence of a multiwavelength thermal/optical carbon analyzer. *Aerosol and Air Quality Research*, *15*(4), 1145–1159. https://doi.org/10.4209/aaqr.2015.02.0106

Chow, J. C., Watson, J. G., Chen, L.-W. A., Chang, M. C. O., Robinson, N. F., Trimble, D., & Kohl, S. (2007). The IMPROVE_A temperature protocol for thermal/optical carbon analysis: Maintaining consistency with a long-term database. *Journal of the Air & Waste Management Association*, *57*(9), 1014–1023. https://doi.org/10.3155/1047-3289.57.9.1014

Chow, J. C., Watson, J. G., Green, M. C., Wang, X., Chen, L. W. A., Trimble, D. L., et al. (2018). Separation of brown carbon from black carbon for IMPROVE and chemical speciation network PM2.5 samples. *Journal of the Air & Waste Management Association*, *68*(5), 494–510. https://doi.org/10.1080/10962247.2018.1426653

Chung, C. E., Ramanathan, V., & Decremer, D. (2012). Observationally constrained estimates of carbonaceous aerosol radiative forcing. *Proceedings of the National Academy of Sciences*, *109*(29), 11,624–11,629. https://doi.org/10.1073/pnas.1203707109

Duncan Fairlie, T., Jacob, D. J., & Park, R. J. (2007). The impact of transpacific transport of mineral dust in the United States. *Atmospheric Environment*, *41*(6), 1251–1266. https://doi.org/10.1016/j.atmosenv.2006.09.048

Eastham, S. D., & Jacob, D. J. (2017). Limits on the ability of global Eulerian models to resolve intercontinental transport of chemical plumes. *Atmospheric Chemistry and Physics*, *17*(4), 2543–2553. https://doi.org/10.5194/acp-17-2543-2017

Feng, Y., Ramanathan, V., & Kotamarthi, V. R. (2013). Brown carbon: A significant atmospheric absorber of solar radiation? *Atmospheric Chemistry and Physics*, *13*(17), 8607–8621. https://doi.org/10.5194/acp-13-8607-2013

Fleming, L. T., Lin, P., Roberts, J. M., Selimovic, V., Yokelson, R., Laskin, J., et al. (2020). Molecular composition and photochemical lifetimes of brown carbon chromophores in biomass burning organic aerosol. *Atmospheric Chemistry and Physics*, *20*(2), 1105–1129. https://doi.org/10.5194/acp-20-1105-2020

Flores, J. M., Zhao, D. F., Segev, L., Schlag, P., Kiendler-Scharr, A., Fuchs, H., et al. (2014). Evolution of the complex refractive index in the UV spectral region in ageing secondary organic aerosol. *Atmospheric Chemistry and Physics*, *14*(11), 5793–5806. https://doi.org/10.5194/acp-14-5793-2014

Forrister, H., Liu, J., Scheuer, E., Dibb, J., Ziemba, L., Thornhill, K. L., et al. (2015). Evolution of brown carbon in wildfire plumes. *Geophysical Research Letters*, *42*(11), 4623–4630. https://doi.org/10.1002/2015GL063897

Giglio, L., Randerson, J. T., & Werf, G. R. van der (2013). Analysis of daily, monthly, and annual burned area using the fourth-generation global fire emissions database (GFED4). *Journal of Geophysical Research: Biogeosciences*, *118*, 317–328. https://doi.org/10.1002/jgrg.20042

He, Q., Bluvshtein, N., Segev, L., Meidan, D., Flores, J. M., Brown, S. S., et al. (2018). Evolution of the complex refractive index of secondary organic aerosols during atmospheric aging. *Environmental Science & Technology*, *52*(6), 3456–3465. https://doi.org/10.1021/acs.est.7b05742

Heald, C. L., Ridley, D. A., Kroll, J. H., Barrett, S. R. H., Cady-Pereira, K. E., Alvarado, M. J., & Holmes, C. D. (2014). Contrasting the direct radiative effect and direct radiative forcing of aerosols. *Atmospheric Chemistry and Physics*, *14*(11), 5513–5527. https://doi.org/10.5194/acp-14-5513-2014

Hecobian, A., Zhang, X., Zheng, M., Frank, N., Edgerton, E. S., & Weber, R. J. (2010). Water-soluble organic aerosol material and the light-absorption characteristics of aqueous extracts measured over the southeastern United States. *Atmospheric Chemistry and Physics*, *10*(13), 5965–5977. https://doi.org/10.5194/acp-10-5965-2010

Jiang, H., Frie, A. L., Lavi, A., Chen, J. Y., Zhang, H., Bahreini, R., & Lin, Y.-H. (2019). Brown carbon formation from nighttime chemistry of unsaturated heterocyclic volatile organic compounds. *Environmental Science & Technology Letters*, *6*(3), 184–190. https://doi.org/10.1021/acs.estlett.9b00017

Jo, D. S., Park, R. J., Lee, S., Kim, S. W., & Zhang, X. (2016). A global simulation of brown carbon: Implications for photochemistry and direct radiative effect. *Atmospheric Chemistry and Physics*, *16*(5), 3413–3432. https://doi.org/10.5194/acp-16-3413-2016

Kirchstetter, T. W., Novakov, T., & Hobbs, P. V. (2004). Evidence that the spectral dependence of light absorption by aerosols is affected by organic carbon. *Journal of Geophysical Research*, *109*, D21208. https://doi.org/10.1029/2004JD004999

Kirchstetter, T. W., & Thatcher, T. L. (2012). Contribution of organic carbon to wood smoke particulate matter absorption of solar radiation. *Atmospheric Chemistry and Physics*, *12*(14), 6067–6072. https://doi.org/10.5194/acp-12-6067-2012

Lack, D. A., Langridge, J. M., Bahreini, R., Cappa, C. D., Middlebrook, A. M., & Schwarz, J. P. (2012). Brown carbon and internal mixing in biomass burning particles. *Proceedings of the National Academy of Sciences*, *109*(37), 14,802–14,807. https://doi.org/10.1073/pnas.1206575109

Lambe, A. T., Cappa, C. D., Massoli, P., Onasch, T. B., Forestieri, S. D., Martin, A. T., et al. (2013). Relationship between oxidation level and optical properties of secondary organic aerosol. *Environmental Science & Technology*, *47*(12), 6349–6357. https://doi.org/10.1021/es401043j

Laskin, A., Laskin, J., & Nizkorodov, S. A. (2015). Chemistry of atmospheric brown carbon. *Chemical Reviews*, *115*(10), 4335–4382. https://doi.org/10.1021/cr5006167

Lee, H. J., Aiona, P. K., Laskin, A., Laskin, J., & Nizkorodov, S. A. (2014). Effect of solar radiation on the optical properties and molecular composition of laboratory proxies of atmospheric brown carbon. *Environmental Science & Technology*, *48*(17), 10,217–10,226. https://doi.org/10.1021/es502515r

Li, C., He, Q., Schade, J., Passig, J., Zimmermann, R., Meidan, D., et al. (2019). Dynamic changes in optical and chemical properties of tar ball aerosols by atmospheric photochemical aging. *Atmospheric Chemistry and Physics*, *19*(1), 139–163. https://doi.org/10.5194/acp-19-139-2019

Lin, G., Penner, J. E., Flanner, M. G., Sillman, S., Xu, L., & Zhou, C. (2014). Radiative forcing of organic aerosol in the atmosphere and on snow: Effects of SOA and brown carbon. *Journal of Geophysical Research: Atmospheres*, *119*, 7453–7476. https://doi.org/10.1002/2013JD021186

Lin, P., Aiona, P. K., Li, Y., Shiraiwa, M., Laskin, J., Nizkorodov, S. A., & Laskin, A. (2016). Molecular characterization of brown carbon in biomass burning aerosol particles. *Environmental Science & Technology*, *50*(21), 11,815–11,824. https://doi.org/10.1021/acs.est.6b03024

McClure, C. D., Lim, C. Y., Hagan, D. H., Kroll, J. H., & Cappa, C. D. (2020). Biomass-burning-derived particles from a wide variety of fuels—Part 1: Properties of primary particles. *Atmospheric Chemistry and Physics*, *20*(3), 1531–1547. https://doi.org/10.5194/acp-20-1531-2020

Molod, A., Salmun, H., & Collow, A. B. M. (2019). Annual cycle of planetary boundary layer heights estimated from wind profiler network data. *Journal of Geophysical Research: Atmospheres*, *124*, 6207–6221. https://doi.org/10.1029/2018JD030102

Pai, S. J., Heald, C. L., Pierce, J. R., Farina, S. C., Marais, E. A., Jimenez, J. L., et al. (2020). An evaluation of global organic aerosol schemes using airborne observations. *Atmospheric Chemistry and Physics*, *20*(5), 2637–2665. https://doi.org/10.5194/acp-20-2637-2020

Park, R. J., Jacob, D. J., Chin, M., & Martin, R. V. (2003). Sources of carbonaceous aerosols over the United States and implications for natural visibility. *Journal of Geophysical Research*, *108*(D12), 4355. https://doi.org/10.1029/2002JD003190

Park, R. J., Jacob, D. J., Field, B. D., Yantosca, R. M., & Chin, M. (2004). Natural and transboundary pollution influences on sulfate-nitrate-ammonium aerosols in the United States: Implications for policy. *Journal of Geophysical Research*, *109*, D15204. https://doi.org/10.1029/2003JD004473

Park, R. J., Kim, M. J., Jeong, J. I., Youn, D., & Kim, S. (2010). A contribution of brown carbon aerosol to the aerosol light absorption and its radiative forcing in East Asia. *Atmospheric Environment*, *44*(11), 1414–1421. https://doi.org/10.1016/j.atmosenv.2010.01.042

Potter, K. M., & Conkling, B. L. (Eds.). (2017). *Forest health monitoring: National status, trends, and analysis 2016. Gen. Tech. Rep. SRS-222* (pp. 1–195). Asheville, NC: U.S. Department of Agriculture, Forest Service, Southern Research Station. Retrieved from https://www.fs.usda.gov/treesearch/pubs/54586

Ridley, D. A., Heald, C. L., Ridley, K. J., & Kroll, J. H. (2018). Causes and consequences of decreasing atmospheric organic aerosol in the United States. *Proceedings of the National Academy of Sciences*, *115*(2), 290–295. https://doi.org/10.1073/pnas.1700387115

Saleh, R. (2020). From measurements to models: Toward accurate representation of brown carbon in climate calculations. *Current Pollution Reports*, *6*(2), 90–104. https://doi.org/10.1007/s40726-020-00139-3

Saleh, R., Marks, M., Heo, J., Adams, P. J., Donahue, N. M., & Robinson, A. L. (2015). Contribution of brown carbon and lensing to the direct radiative effect of carbonaceous aerosols from biomass and biofuel burning emissions. *Journal of Geophysical Research: Atmospheres*, *120*, 10,285–10,296. https://doi.org/10.1002/2015JD023697

Saleh, R., Robinson, E. S., Tkacik, D. S., Ahern, A. T., Liu, S., Aiken, A. C., et al. (2014). Brownness of organics in aerosols from biomass burning linked to their black carbon content. *Nature Geoscience*, *7*(9), 647–650. https://doi.org/10.1038/ngeo2220

Schuster, G. L., Dubovik, O., Arola, A., Eck, T. F., & Holben, B. N. (2016). Remote sensing of soot carbon—Part 2: Understanding the absorption Ångström exponent. *Atmospheric Chemistry and Physics*, *16*(3), 1587–1602. https://doi.org/10.5194/acp-16-1587-2016

Sumlin, B. J., Pandey, A., Walker, M. J., Pattison, R. S., Williams, B. J., & Chakrabarty, R. K. (2017). Atmospheric photooxidation diminishes light absorption by primary brown carbon aerosol from biomass burning. *Environmental Science & Technology Letters*, *4*(12), 540–545. https://doi.org/10.1021/acs.estlett.7b00393

van der Werf, G. R., Randerson, J. T., Giglio, L., Collatz, G. J., Mu, M., Kasibhatla, P. S., et al. (2010). Global fire emissions and the contribution of deforestation, savanna, forest, agricultural, and peat fires (1997–2009). *Atmospheric Chemistry and Physics*, *10*(23), 11,707–11,735. https://doi.org/10.5194/acp-10-11707-2010

Wang, X., Heald, C. L., Liu, J., Weber, R. J., Campuzano-Jost, P., Jimenez, J. L., et al. (2018). Exploring the observational constraints on the simulation of brown carbon. *Atmospheric Chemistry and Physics*, *18*(2), 635–653. https://doi.org/10.5194/acp-18-635-2018

Wang, X., Heald, C. L., Ridley, D. A., Schwarz, J. P., Spackman, J. R., Perring, A. E., et al. (2014). Exploiting simultaneous observational constraints on mass and absorption to estimate the global direct radiative forcing of black carbon and brown carbon. *Atmospheric Chemistry and Physics*, *14*(20), 10,989–11,010. https://doi.org/10.5194/acp-14-10989-2014

Wang, X., Heald, C. L., Sedlacek, A. J., de Sá, S. S., Martin, S. T., Alexander, M. L., et al. (2016). Deriving brown carbon from multiwavelength absorption measurements: Method and application to AERONET and Aethalometer observations. *Atmospheric Chemistry and Physics*, *16*(19), 12,733–12,752. https://doi.org/10.5194/acp-16-12733-2016

Warneke, C., Bahreini, R., Brioude, J., Brock, C. A., Gouw, J. A., Fahey, D. W., et al. (2009). Biomass burning in Siberia and Kazakhstan as an important source for haze over the Alaskan Arctic in April 2008. *Geophysical Research Letters*, *36*, L02813. https://doi.org/10.1029/2008GL036194

Warton, D. I., Wright, I. J., Falster, D. S., & Westoby, M. (2006). Bivariate line-fitting methods for allometry. *Biological Reviews*, *81*(2), 259–291. https://doi.org/10.1017/S1464793106007007

Zeng, L., Zhang, A., Wang, Y., Wagner, N. L., Katich, J. M., Schwarz, J. P., et al. (2020). Global measurements of brown carbon and estimated direct radiative effects. *Geophysical Research Letters*, *47*, e2020GL088747. https://doi.org/10.1029/2020GL088747

Zhang, A., Wang, Y., Zhang, Y., Weber, R. J., Song, Y., Ke, Z., & Zou, Y. (2020). Modeling the global radiative effect of brown carbon: A potentially larger heating source in the tropical free troposphere than black carbon. *Atmospheric Chemistry and Physics*, *20*(4), 1901–1920. https://doi.org/10.5194/acp-20-1901-2020

Zhang, X., Kim, H., Parworth, C. L., Young, D. E., Zhang, Q., Metcalf, A. R., & Cappa, C. D. (2016). Optical properties of wintertime aerosols from residential wood burning in Fresno, CA: Results from DISCOVER-AQ 2013. *Environmental Science & Technology*, *50*(4), 1681–1690. https://doi.org/10.1021/acs.est.5b04134

Zhang, X., Lin, Y.-H., Surratt, J. D., & Weber, R. J. (2013). Sources, composition and absorption Ångström exponent of light-absorbing organic components in aerosol extracts from the Los Angeles Basin. *Environmental Science & Technology*, *47*(8), 3685–3693. https://doi.org/10.1021/es305047b

Zhang, X., Lin, Y.-H., Surratt, J. D., Zotter, P., Prévôt, A. S. H., & Weber, R. J. (2011). Light-absorbing soluble organic aerosol in Los Angeles and Atlanta: A contrast in secondary organic aerosol. *Geophysical Research Letters*, *38*, L21810. https://doi.org/10.1029/2011GL049385

Zhang, Y., Forrister, H., Liu, J., Dibb, J., Anderson, B., Schwarz, J. P., et al. (2017). Top-of-atmosphere radiative forcing affected by brown carbon in the upper troposphere. *Nature Geoscience*, *10*. https://doi.org/10.1038/ngeo2960

Zhao, R., Lee, A. K. Y., Huang, L., Li, X., Yang, F., & Abbatt, J. P. D. (2015). Photochemical processing of aqueous atmospheric brown carbon. *Atmospheric Chemistry and Physics*, *15*(11), 6087–6100. https://doi.org/10.5194/acp-15-6087-2015

Zhong, M., & Jang, M. (2014). Dynamic light absorption of biomass-burning organic carbon photochemically aged under natural sunlight. *Atmospheric Chemistry and Physics*, *14*(3), 1517–1525. https://doi.org/10.5194/acp-14-1517-2014

EPA NEI (2015). National Emissions Inventory (NEI) Air Pollutant Emissions Trends Data. https://www.epa.gov/air-emissions-inventories/air-pollutant-emissionstrends-data

References From the Supporting Information

Chakrabarty, R. K., Gyawali, M., Yatavelli, R. L. N., Pandey, A., Watts, A. C., Knue, J., et al. (2016). Brown carbon aerosols from burning of boreal peatlands: Microphysical properties, emission factors, and implications for direct radiative forcing. *Atmospheric Chemistry and Physics*, *16*(5), 3033–3040. https://doi.org/10.5194/acp-16-3033-2016

Cheng, Y., He, K.-B., Zheng, M., Duan, F.-K., Du, Z.-Y., Ma, Y.-L., et al. (2011). Mass absorption efficiency of elemental carbon and water-soluble organic carbon in Beijing, China. *Atmospheric Chemistry and Physics*, *11*(22), 11,497–11,510.

Corr, C. A., Hall, S. R., Ullmann, K., Anderson, B. E., Beyersdorf, A. J., Thornhill, K. L., et al. (2012). Spectral absorption of biomass burning aerosol determined from retrieved single scattering albedo during ARCTAS. *Atmospheric Chemistry and Physics*, *12*(21), 10,505–10,518. https://doi.org/10.5194/acp-12-10505-2012

Dasari, S., Andersson, A., Bikkina, S., Holmstrand, H., Budhavant, K., Satheesh, S., et al. (2019). Photochemical degradation affects the light absorption of water-soluble brown carbon in the South Asian outflow. *Science Advances*, *5*(1), eaau8066. https://doi.org/10.1126/sciadv.aau8066

Hoffer, A., Gelencser, A., Guyon, P., Kiss, G., Schmid, O., Frank, G. P., et al. (2006). Optical properties of humic-like substances (HULIS) in biomass-burning aerosols. *Atmospheric Chemistry and Physics*, *8*. https://doi.org/10.5194/acp-6-3563-2006

Liu, J., Bergin, M., Guo, H., King, L., Kotra, N., Edgerton, E., & Weber, R. J. (2013). Size-resolved measurements of brown carbon in water and methanol extracts and estimates of their contribution to ambient fine-particle light absorption. *Atmospheric Chemistry and Physics*, *13*(24), 12,389–12,404. https://doi.org/10.5194/acp-13-12389-2013

Liu, J., Scheuer, E., Dibb, J., Diskin, G. S., Ziemba, L. D., Thornhill, K. L., et al. (2015). Brown carbon aerosol in the North American continental troposphere: Sources, abundance, and radiative forcing. *Atmospheric Chemistry and Physics*, *15*(14), 7841–7858. https://doi.org/10.5194/acp-15-7841-2015

Liu, J., Scheuer, E., Dibb, J., Ziemba, L. D., Thornhill, K. L., Anderson, B. E., et al. (2014). Brown carbon in the continental troposphere. *Geophysical Research Letters*, *41*, 2191–2195. https://doi.org/10.1002/2013GL058976

McNaughton, C. S., Clarke, A. D., Freitag, S., Kapustin, V. N., Kondo, Y., Moteki, N., et al. (2011). Absorbing aerosol in the troposphere of the Western Arctic during the 2008 ARCTAS/ARCPAC airborne field campaigns. *Atmospheric Chemistry and Physics*, *11*(15), 7561–7582. https://doi.org/10.5194/acp-11-7561-2011

Pokhrel, R. P., Wagner, N. L., Langridge, J. M., Lack, D. A., Jayarathne, T., Stone, E. A., et al. (2016). Parameterization of single-scattering albedo (SSA) and absorption Ångström exponent (AAE) with EC/OC for aerosol emissions from biomass burning. *Atmospheric Chemistry and Physics*, *16*(15), 9549–9561. https://doi.org/10.5194/acp-16-9549-2016

Srinivas, B., & Sarin, M. M. (2013). Light absorbing organic aerosols (brown carbon) over the tropical Indian Ocean: Impact of biomass burning emissions. *Environmental Research Letters*, *8*(4), 044042. https://doi.org/10.1088/1748-9326/8/4/044042

Srinivas, B., & Sarin, M. M. (2014). Brown carbon in atmospheric outflow from the Indo-Gangetic Plain: Mass absorption efficiency and temporal variability. *Atmospheric Environment*, *89*, 835–843. https://doi.org/10.1016/j.atmosenv.2014.03.030

Sun, H., Biedermann, L., & Bond, T. C. (2007). Color of brown carbon: A model for ultraviolet and visible light absorption by organic carbon aerosol. *Geophysical Research Letters*, *34*, L17813. https://doi.org/10.1029/2007GL029797

Wu, G., Ram, K., Fu, P., Wang, W., Zhang, Y., Liu, X., et al. (2019). Water-soluble brown carbon in atmospheric aerosols from Godavari (Nepal), a regional representative of South Asia. *Environmental Science & Technology*, *53*(7), 3471–3479. https://doi.org/10.1021/acs.est.9b00596

Yang, M., Howell, S. G., Zhuang, J., & Huebert, B. J. (2009). Attribution of aerosol light absorption to black carbon, brown carbon, and dust in China—Interpretations of atmospheric measurements during EAST-AIRE. *Atmospheric Chemistry and Physics*, *9*(6), 2035–2050. https://doi.org/10.5194/acp-9-2035-2009